

# Solvation Dynamics in Water. 2. Energy fluxes on excited and ground state surfaces

Rosend Rey\*

*Departament de Física, Universitat Politècnica de Catalunya, Campus Nord B4-B5, Barcelona 08034, Spain.*

James T. Hynes†

*Department of Chemistry and Biochemistry University of Colorado, Boulder, CO 80309-0215 USA,  
Ecole Normale Supérieure-PSL Research University,  
Chemistry Department, Sorbonne Universités-UPMC University Paris 06,  
CNRS UMR 8640 Pasteur, 24 rue Lhomond, 75005 Paris, FR*

(Dated: September 5, 2016)

This series' first installment introduced an approach to solvation dynamics focused on expressing the emission frequency shift (following electronic excitation of, and resulting charge change or redistribution in, a solute) in terms of energy fluxes, a work and power perspective. This approach, which had been previously exploited for rotational and vibrational excitation-induced energy flow, has the novel advantage of providing a quantitative view and understanding of the molecular level mechanisms involved in the solvation dynamics, via tracing of the energy flow induced by the electronic excitation's charge change or redistribution in the solute. This new methodology, which was illustrated for the case in which only the excited electronic state surface contributes to the frequency shift (ionization of a monatomic solute in water), is here extended to the general case, in which both the excited and ground electronic states may contribute. Simple monatomic solute model variations allow discussion of the (sometimes surprising) issues involved in assessing each surface's contribution. The calculation of properly defined energy fluxes/work allows a more complete understanding of the solvation dynamics even when the real work for one of the surfaces does not directly contribute to the frequency shift, an aspect further emphasizing the utility of an energy flux approach.

**Keywords:** Energy transfer, frequency shift, librations, ion hydration, solvent relaxation.

## I. INTRODUCTION

In Ref. 1 (hereafter denoted as I) we addressed from a novel work and power perspective the calculation of the time-dependent frequency shift that follows electronic excitation of a chromophore embedded in a solvent<sup>2-10</sup>, i.e. the time-dependent Stokes shift (TDSS). It was shown for a model system how this shift can be usefully formulated in terms of the flow of excess energy induced by the solute charge change or redistribution resulting from the electronic excitation into solute and solvent configurational degrees of freedom. This approach's primary benefit is that it provides direct information on the microscopic mechanisms involved in the relaxation beyond the usual but more limited perspective, e.g. the behavior of energy gap time correlation functions. This is an important issue, since TDSS studies have as one key goal the provision of insight for solvation dynamics of relevance for chemical reactions, and the channeling of energy in chemical reaction pathways which depend on translational, rotational, and vibrational modes of the solvent not explicitly revealed in traditional TDSS studies. Several previous reports have shown that this energy flow approach results in a clear-cut understanding of molecular mechanisms involved in rotational/librational and vibrational relaxation of neat liquid water.<sup>14-16</sup> (The rotations in liquid water are of course hindered rotations, i.e. librations; we will use both appellations).

In our first application of this methodology to the solvation dynamics issue, the system selected for study was extremely simple in its solute choice: a neutral

monatomic solute in liquid water that acquires a unit (positive or negative) charge, at fixed solute size, after electronic excitation; in fact, this choice was almost compulsory given extensive previous attention devoted to it.<sup>17-29</sup> Thanks to this system's simplicity, the frequency shift is identical to the excited state ion-water solvent Coulomb energy. Consequently, the resulting excess energy's time variation could be readily expressed in terms of a sum of contributions of work on the solvent (and solute) configurational degrees of freedom. This constitutes the core of the work/power approach, since this additive character allows scrutiny of the different channels for the energy transfer and relaxation that accompany the frequency red shift. The resulting quantitative estimations of the modes of motion/molecules and energy transfer routes involved in the relaxation process, went far beyond the more common indirect and qualitative estimations allowed by normalized equilibrium frequency shift time correlation functions or even nonequilibrium shift simulations. In addition, a number of non-trivial common traits were revealed, including the largely charge-independent relative weights of energy transferred into hindered rotations/translations, or into different body-fixed rotational axes for the rotational channel.

The aforementioned attractive features motivate the investigation of a wider set of systems; this requires generalization of the computational approach in order to take into account that—in contrast to the simple systems studied in I—both electronic surfaces may be characterized by non-zero charge distributions and thus contribute to the frequency shift, which of course is by far the most common occurrence in reality. The frequency shift can

still be expressed in terms of certain work contributions, now with contributions from both the excited and ground states. These two contributions can be calculated via straightforward simulations.

But our aim goes far beyond the simple issue of calculation via simulation; it is to decompose these work contributions in terms of real molecular energy fluxes associated with solvent hindered rotations and translations and to identify actual energy flow paths associated with the frequency shift dynamics, and it is here that a complication arises. Briefly stated, the actual dynamics occurring in the water solvent relaxation subsequent to the excitation is that on the excited electronic state surface, i.e. with the excited electronic state Hamiltonian involving the excited state solvent interacting with the solvent. The first work contribution to the frequency shift explicitly involves the interactions on the excited state solute with the solvent, both governed by those dynamics; the energy flow involved is associated with the real dynamics occurring in the excited state. But a second contribution involves the *ground state* solute interacting with the solvent, whose evolution is governed by the *excited state* dynamics, i.e. the dynamics governed by the excited state solute’s charge and not by the ground state solute’s charge. The latter cases’ solute-dynamics mismatch makes the work involved—although mathematically well-defined—a virtual work, as opposed to the real work character of the first contribution in which the solute and dynamics coincide, i.e. are both excited state. Approximately half of this article will be concerned with a detailed analysis of these issues and the construction of an approach such that the virtual work just mentioned is usefully approximated by a real work contribution—thus allowing a molecular frequency shift analysis of molecular level energy flow mechanisms associated with both ground and electronic states.

Since the present effort explores the energy flux perspective for the generalized case of excited and ground state participation in solvation dynamics, it is of interest—and will prove instructive—to investigate some idealized scenarios that probe the limits of the methodology. We have already emphasized that some issues that can arise for the frequency shift. Beyond that, a perspective beyond the exclusive focus on that shift can be of interest. Thus, although the dissection of the computed frequency shift in terms of energy fluxes provides a substantial amount of information about the nonequilibrium solvation dynamics, in some cases part of the process might be missing in that shift. This can be illustrated by two examples, now discussed.

In the first example, a charged ground state solute is excited to a neutral solute excited state. The ensuing excited state dynamics involves the solvent evolving in the presence of that neutral solute. But there are no Coulomb forces between the neutral solute and the water solvent, so that this real evolution situation does not govern the frequency shift (which instead is governed by the ground state interactions). A second, although less

dramatic, example is provided by the case of a neutral solute that upon excitation acquires a unit charge, i.e. the simple systems of I. While the frequency shift reflects the time evolution of the ion-solvent Coulomb energy on the excited state, in the actual process the solute makes a transition to the neutral ground state in a trajectory, with the emission of a photon of the appropriate frequency. Now there is a solvent relaxation of the ground electronic state: upon this transition, the solvent is in a highly nonequilibrium state vis a vis the ground state solute. Once the solute charge has been switched off, strong uncompensated repulsion forces will remain among the first (and further) shell hydration molecules, and these forces will give rise to fast solvation dynamics. But this solvent relaxation is not directly followed by the frequency shift relaxation, which is governed by the excited state dynamics. Indeed, since there are no direct (now) neutral solute-solvent Coulomb forces, the Coulomb work on that ground state solute vanishes. As will be shown, even this special scenario problem can be handled by monitoring energy fluxes, albeit now involving the total potential energy of the whole system (as opposed to involving solely the solute-solvent Coulomb energy). This approach can also provide an alternative perspective for cases where frequency shift analysis would be regarded as sufficient in a standard perspective. The second half of this contribution focuses on these aspects.

The outline of the remainder of this paper is as follows. In the following section, we briefly summarize the systems and parameters used in the simulations. The analysis of the frequency shift for general systems is described in Sec. III, including approximation of virtual work terms by real work terms, while Sec. IV presents the alternative perspective to solvation dynamics just described. Finally, concluding remarks are offered in Sec. V.

## II. COMPUTATIONAL DETAILS

We again use the simple model systems of the type employed in I. Given the negligible contribution of internal solvent vibrations reported in I, here we only consider the (rigid) SPC/E model<sup>30</sup> for the solvent water molecules. For the solute we have adopted (as in I) the same choices as Tran and Schwartz<sup>25</sup> for ease of comparison. Water-solute interaction consists of a Lennard-Jones interaction identical to the water-water LJ interaction (this water model does not include LJ terms associated with the hydrogens), plus Coulomb interactions which depend on the solute charge (neutral, or positive/negative unit charge).

All simulations have been run with an in-house code for a single solute and 199 water molecules, which for a cut-off distance of half the box length corresponds to an interaction length of 9 Å. The Ewald sum correction has been included for Coulomb forces. The simulations consist of a long trajectory from which initial configurations are sampled. The latter are used for independent separate

nonequilibrium runs, where the solute charge is changed at  $t = 0$ , and along which the quantities of interest are calculated. Temperature control is maintained<sup>31</sup> during the generation of initial configurations, and turned off at each non-equilibrium trajectory's start. Further details will be reported when required.

An important issue, addressed here and in I, is the extent to which solvation dynamics is collective. In this connection we have found it useful to separate the contribution of the different hydration layers. It was argued in I that it is possible to construct a unique definition of hydration shells which reasonably accommodates rather different structures around the solute, namely those corresponding to neutral and positive/negative ions. The first shell has been defined as enclosing all water molecules up to a maximum distance of 3.9 Å, a radius which on average contains roughly eight water molecules irrespective of the solute charge. For the second shell the distance chosen is 6.0 Å, so that both shells contain a total of roughly thirty water molecules on average.

### III. FREQUENCY SHIFT AND WORK

#### A. Theory

The approach followed in I focused on a monatomic solute which can be in either of two electronic states: a neutral ground state and an excited charged state. Now we are interested in the general case, for which both the ground ( $gs$ ) and the excited state ( $es$ ) are characterized by finite charge distributions. The Hamiltonians including the solvent are, respectively,

$$H_{gs} = K + H_{gs}^0 + H_s + U_{gs,s}, \quad (1)$$

$$H_{es} = K + H_{es}^0 + H_s + U_{es,s}. \quad (2)$$

The first two terms correspond in each case to the contribution associated with the unperturbed solute:  $K$  denotes the solute kinetic energy, and  $(H_{gs}^0, H_{es}^0)$  are the constant electronic energies in the ground and excited states respectively, so that the unperturbed transition energy is given by

$$\hbar\omega_0 = H_{es}^0 - H_{gs}^0. \quad (3)$$

Inclusion of solute internal modes is formally similar to the monatomic solute case, as pointed out below.

Returning to Eqs. 1,2, the solvent kinetic and potential energies are grouped into a single term ( $H_s$ ). Finally, the terms  $(U_{gs,s}, U_{es,s})$  correspond to the solute-solvent interactions in the solute ground and excited states respectively. In the present model, the interaction is represented by Lennard-Jones ( $V^{LJ}$ ) and Coulomb ( $V^c$ ) interactions between the solvent molecules and the solute. Assuming throughout that only the Coulomb interactions change upon solute excitation, for a given solvent config-

uration we will have

$$\Delta E(t) \equiv H_{es}(t) - H_{gs}(t) = [V_{es,s}^c(t) - V_{gs,s}^c(t)] + \hbar\omega_0, \quad (4)$$

which shows that, as expected, the instantaneous frequency shift  $\delta\hbar\omega(t) \equiv \Delta E(t) - \hbar\omega_0$  is given solely by the instantaneous energy gap, here the difference in Coulomb energy between the excited ( $V_{es,s}^c$ ) and ground ( $V_{gs,s}^c$ ) states. (In order to include solute internal vibrations we would only need to add the difference in the solute's configurational internal energy between its excited and ground state.)

The time-dependent average frequency shift can thus be determined as a nonequilibrium average  $s(t)$  (denoted by over-bars), computed over a set of trajectories

$$s(t) \equiv \overline{\delta\hbar\omega(t)} = \overline{V_{es,s}^c(t) - V_{gs,s}^c(t)} \equiv \overline{\delta V^c(t)}. \quad (5)$$

Consequently, the normalized frequency shift, which is the usual focus of interest, can also be expressed in terms of Coulomb energies as well

$$S(t) \equiv \frac{\overline{\delta\hbar\omega(t)} - \overline{\delta\hbar\omega(\infty)}}{\overline{\delta\hbar\omega(0)} - \overline{\delta\hbar\omega(\infty)}} = \frac{\overline{\delta V^c(t)} - \overline{\delta V^c(\infty)}}{\overline{\delta V^c(0)} - \overline{\delta V^c(\infty)}}. \quad (6)$$

We now turn to the relation of the above standard formulation with our power/work/energy flux perspective. As detailed in Refs. 14,15, the motivation for an approach based on the computation of energy fluxes (power) stems from the fact that these fluxes can be disentangled in terms of the contributions from each molecule and its degrees of freedom. We start the formulation by noting that, according to Eq. 5, the frequency shift can be expressed as the time evolution of the Coulomb energy gap  $\delta V^c(t)$  over nonequilibrium trajectories evolving on the excited state surface. The Hamiltonian that drives this excited state dynamics is (without constant terms)

$$H = K_{solute} + V_{es,s}^c + V^{LJ} + K_{solvent} + U_{solvent}, \quad (7)$$

where the last two terms correspond to the Hamiltonian  $H_s$  in Eqs. 1 and 2.

The time derivative of the quantity of interest ( $\delta V^c(t)$ ) can be expressed in terms of Poisson brackets<sup>15</sup> as

$$\begin{aligned} \frac{d\delta V^c}{dt} &= [\delta V^c, H] = [\delta V^c, K] = \\ &= [V_{es}^c, K] - [V_{gs}^c, K] = \\ &= \sum_i \left( \frac{\partial V_{es}^c}{\partial x_i} \frac{\partial K}{\partial p_i} - \frac{\partial V_{gs}^c}{\partial x_i} \frac{\partial K}{\partial p_i} \right) = \\ &= - \sum_j \left( \vec{F}_j^{es,s} - \vec{F}_j^{gs,s} \right) \cdot \vec{v}_j \end{aligned} \quad (8)$$

here the index  $i$  runs over spatial coordinates of all interaction sites, while  $j$  only runs over interactions sites.

The set  $\{\vec{F}_j^{es,s}\}$  denotes the excited state Coulomb forces on site  $j$ , either on the solute or solvent. Note that

this Coulomb force is not the total Coulomb force acting on the site, since it does not include solvent-solvent Coulomb interactions. In addition —and this is the point that differs from our previous discussion in I— we also have now the set of forces  $\{\vec{F}_j^{gs,s}\}$ . These are “virtual” forces since they correspond to the forces that would be exerted when the solute has the charge distribution corresponding to its ground state, but the dynamics of the solvent is that in the excited state, i.e. in the presence of the excited state solute’s charge distribution. This is the solute-solvent dynamics mismatch we discussed in the Introduction, and we discuss it further below.

For the solvation dynamics/relaxation problem focused on the frequency shift dynamics, we need, as required by Eq. 6, the integrated result  $\delta V^c(t)$ , which is straightforward from Eq. 8,

$$\Delta V^c(t) \equiv \delta V^c(t) - \delta V^c(0) = -W^{es|es}(t) + W^{gs|es}(t), \quad (9)$$

where the first term  $W^{es|es}$  on the rhs corresponds to the real work performed at time  $t$  after the initial ground to excited state transition; the first superscript label indicates that the solute has the excited state ( $es$ ) charge distribution and the second label ( $es$ ) indicates that the dynamics is excited state dynamics, i.e. the solvent interacts with the  $es$  solute charge distribution. More explicitly,  $W^{es|es}(t)$  is

$$W^{es|es}(t) = \sum_j \int_0^t \vec{F}_j^{es,s|es} \cdot \vec{v}_j dt = \sum_j \int_{\vec{r}_j(0)}^{\vec{r}_j(t)} \vec{F}_j^{es,s|es} \cdot d\vec{r}_j, \quad (10)$$

where we have augmented the force notation to read  $\vec{F}_j^{es,s|es}$  in order to indicate this is the  $es$  solute-solvent force with the solvent dynamics being the  $es$  dynamics ( $|es$  portion of the superscript). We momentarily pause to note that the increment ( $\Delta V^c(t)$ ) defined by Eq. 9 will constitute our main focus of interest since, similarly to what was done in I, it can be easily shown that Eq. 6 for the nonequilibrium averaged and normalized frequency shift can be written

$$S(t) = \frac{\overline{\delta V^c(t)} - \overline{\delta V^c(\infty)}}{\overline{\delta V^c(0)} - \overline{\delta V^c(\infty)}} = \frac{\overline{\Delta V^c(t)}}{\overline{\delta V^c(0)} - \overline{\delta V^c(\infty)}} + 1, \quad (11)$$

which in its second line provides the explicit connection to the nonequilibrium average Coulomb interaction shift, whose numerical evaluation will subsequently be displayed in various figures.

The second term on the rhs of Eq. 9 denotes the virtual work  $W^{gs|es}$  involving the virtual force: the work that would be performed for the solute with the ground state ( $gs$ ) charge distribution (indicated by first superscript label  $gs$ ), but evolving along the real excited state trajectory dictated by the solute with its excited state charge distribution (indicated by the second superscript label

$es$ ). This mismatch between the solute present and the dynamics involved is in complete contrast to the solute-dynamics consistency for the real work Eq. 10.

We emphasize that, from the purely computational point of view, the computation of both work contributions (real and virtual) to the frequency shift presents no difficulty. However, as stressed in the Introduction, we desire a frequency shift formulation in terms of energy flux terms associated with real solvent rotational and translational motions and energy flow mechanisms. The real work, Eq. 10, can be so decomposed directly, but an approximation for the virtual work in Eq. 9 in terms of a real work is required to effect such a decomposition; the approximation required is to attain a consistency between the solute present and the solvent dynamics.

We can begin the construction of an approximate perspective which provides such real work by inverting the limits of the integral that defines the virtual work  $W^{gs|es}$

$$\begin{aligned} W^{gs|es}(t) &= \sum_j \int_0^t \vec{F}_j^{gs,s|es} \cdot \vec{v}_j dt = \quad (12) \\ &= \sum_j \int_{\vec{r}_j(0)}^{\vec{r}_j(t)} \vec{F}_j^{gs,s|es} \cdot d\vec{r}_j = \\ &= - \sum_j \int_{\vec{r}_j(t)}^{\vec{r}_j(0)} \vec{F}_j^{gs,s|es} \cdot d\vec{r}_j. \end{aligned}$$

$W^{gs|es}$  is (minus) the *virtual* work done if at time  $t$  the  $es$  solute would make a transition to its ground state,  $gs$  charge distribution, along the reversed excited state trajectories, i.e. for both the  $es$  solute and solvent with  $es$  dynamics. This reversal has now expressed the integral in the direction of relaxation back towards the initial conditions before the excitation. We now make the approximation to convert this term to a purely ground state relaxation from point B to A (see Fig. 1) by replacing the  $es$  dynamics by the  $gs$  dynamics, this approximation is made solely for the nonequilibrium average and is discussed further below,

$$\begin{aligned} \overline{W^{gs|es}(t)} &= - \overline{\sum_j \int_{\vec{r}_j(t)}^{\vec{r}_j(0)} \vec{F}_j^{gs,s|es} \cdot d\vec{r}_j} \quad (13) \\ &\cong - \overline{\sum_j \int_{\vec{r}_j(t)}^{\vec{r}_j(0)} \vec{F}_j^{gs,s|gs} \cdot d\vec{r}_j} \equiv -\overline{W_{inv}^{gs|gs}(t)} \end{aligned}$$

In this approximate perspective the frequency shift can be rewritten (see Eq. 9) as

$$\overline{\Delta V^c(t)} \cong -\overline{W^{es|es}(t)} - \overline{W_{inv}^{gs|gs}(t)}. \quad (14)$$

We note that some equations hold exactly for each single nonequilibrium trajectory (like Eqs. 1-4,10,12), while others (such as Eqs. 11,13,14), carrying overbar notation, are explicitly intended as expressions for averages over nonequilibrium trajectories. Obviously quantities of experimental interest require such nonequilibrium

averages—see e.g. the basic formula Eq. 5. But the overbar notation for this quickly becomes rather heavy, and to lighten the notation, we will drop the overbars from this point on, with the understanding that we will be exclusively dealing with non-equilibrium averages (as opposed to single trajectories).

A summary can be found in the schematic Fig. 1, which graphically depicts the time evolution of the nonequilibrium averaged shift  $\delta V^c(0)$  created after the initial excitation-induced transition (vertical thin arrow). At time  $t$  it has redshifted ( $\delta V^c(t) < \delta V^c(0)$ ) by an amount *exactly* equal to the nonequilibrium average work performed on configurational degrees of freedom while the solute stays in its excited state ( $W^{es|es}(t)$ , upper thick arrow), plus the virtual work ( $W^{gs|es}$ , upward lower thin arrow) from points A to B; points A and B refer to location on the abscissa progress axis, and do not refer explicitly to either the ground or excited electronic states. This latter work is approximated in Eq. 13 in terms of the average work that would be performed if the solute were to make an electronic transition down to its ground state at that instant (dashed line) and then relax with ground state dynamics (thick solid line from B to A). This approximate average work  $W_{inv}^{gs|gs}$  is the one performed along the ground state trajectories that would bring the solvent back to the ground state initial equilibrium previous to electronic excitation. The approximate expression for the nonequilibrium average shift Eq. 14 involves relaxation in the excited state towards equilibrium with the *es* solute and relaxation in the ground state towards equilibrium with the *gs* solute.

The approximation of one electronic state’s dynamics by the other state’s dynamics in Eq. 13—which allows the frequency shift Eq.5 to be expressed exclusively in terms of real work contributions—is quite similar in character to approximations commonly used in “linear response theory” discussions of the frequency shift, particularly in a time correlation function context.<sup>1–14,17,26,32,33</sup> We will see in Section III C that the approximation works reasonably well even for the relatively challenging<sup>17</sup> case of a single localized charge extinction.

Equation 14 shows that the experimental frequency shift can be understood (approximately) in terms of a sum of two real work contributions. Now since each of these contributions can be partitioned into specific real energy fluxes, valuable information about the participation of the various degrees of freedom may be extracted. For a monatomic solute, each work term can be easily partitioned if we consider that the laboratory velocity of a site ( $i_a$ ) within a given water molecule ( $i$ ) is given by

$$\vec{v}_{i_a} = \vec{v}_i^{CM} + \vec{\omega}_i \times \vec{r}_{i_a} + \vec{v}_{i_a}^v, \quad (15)$$

where  $\vec{v}_i^{CM}$  denotes the center of mass translational velocity,  $\vec{\omega}_i \times \vec{r}_{i_a}$  the rotational velocity, and  $\vec{v}_{i_a}^v$  corresponds to the vibrational velocity in the Eckart frame (see I). If this expression for the velocity is inserted into Eq. 8, after integration we find that each one of the work terms

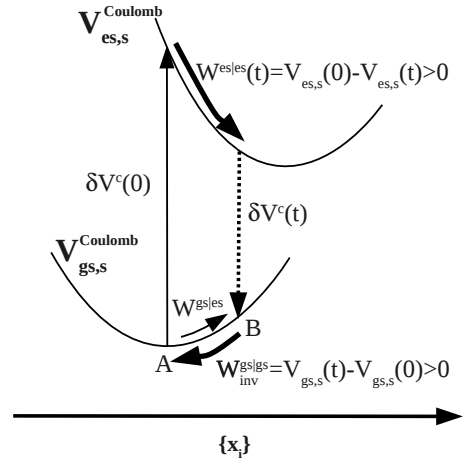


FIG. 1: Schematic sketch of the basic quantities entering the calculation of the frequency shift as described in the text, for a typical excited state trajectory, in an averaged representation. The overbar notation indicating averages is suppressed for visual clarity. Gas phase electronic energies ( $H_{gs}^0, H_{es}^0$ ) have been subtracted from each state and only instantaneous Coulomb energies are represented. The horizontal coordinate  $\{x_i\}$  stands for the system’s multidimensional spatial configuration. As discussed in the text, the nonequilibrium average  $A \rightarrow B$  contribution of the ground state can be approximated, via Eq. 14, in terms of the reverse  $B \rightarrow A$ , real nonequilibrium average relaxation process with ground state solute and ground state dynamics. See the text for further discussion.

(either real—*es|es* or *gs|gs*— or virtual—*gs|es*), that enter Eqs. 10–13 for the frequency shift, can be expressed in terms of a sum of work contributions, which are real or virtual depending upon the situation discussed

$$W(t) = W_{solute}^T(t) + \sum_i W_i^T(t) + \sum_i W_i^R(t) + \sum_i W_i^V(t), \quad (16)$$

i.e. energy transfer into different modes: rotation of each solvent molecule ( $W_i^R$ ), translation of the solute ( $W_{solute}^T$ ) or solvent molecules ( $W_i^T$ ) and, for flexible solvent molecules, intramolecular vibrations ( $W_i^V$ ).

## B. An extreme case illustration

At this stage, we could consider a reasonably straightforward illustration—in which the ground and excited state solutes have differing finite charges—of the real excited state work Eq. 10 and the real work approximation for the ground state Eq. 13, the associated frequency shift Eq. 5 approximated by Eq. 14, and the associated work decompositions Eq. 16. Instead, we will examine the simpler but extreme case mentioned in the Introduction, in which the ground state solute is charged and the excited state is neutral, i.e. the transition  $q = +1 \rightarrow q = 0$ . This case has the merit of starkly illustrating two important aspects. First, the real work in the excited state Eq. 10 vanishes since there is no

Coulomb interaction between the neutral  $es$  solute and the water solvent. This leaves solely the virtual ground state work and its real approximation Eq. 13 to be considered. Second, the frequency shift is determined solely by the virtual ground state work, whose approximation in terms of a real ground state work can be examined; from Eqs. 5 and 14, the shift for this extreme example is given by

$$\Delta V^c(t) = -W^{gs|es}(t) \sim -W_{inv}^{gs|gs}(t). \quad (17)$$

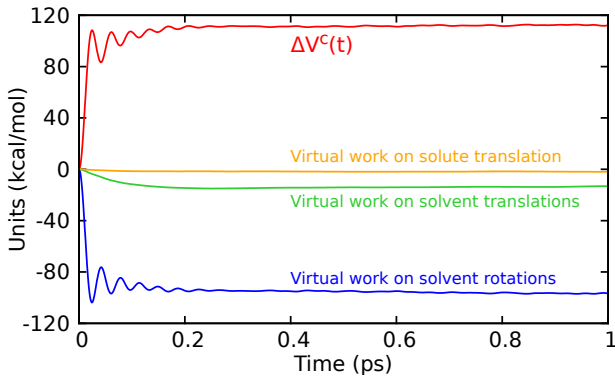


FIG. 2: The frequency shift, the nonequilibrium average  $\Delta V^c(t) = -W^{gs|es}(t)$ , Eq. 12, and the various average contributions to the virtual work  $W^{gs|es}(t)$ . (Overbar notation for nonequilibrium averages in this caption and in the the Figure is suppressed). All of these functions are computed along and averaged over excited state trajectories for the transition  $q = 1 \rightarrow q = 0$ , and rigid water solvent. (The approximation involving the real work  $W_{inv}^{gs|gs}(t)$  will be considered in Fig.3 below).

Figure 2 displays, for the  $q = +1 \rightarrow q = 0$  transition case, the frequency shift energy  $\Delta V^c(t)$  (see Eq. 17) and the partition of the virtual work  $W^{gs|es}(t)$  (see Eq. 17) into its contributions Eq. 16 from molecular translations and hindered rotations. The process involved corresponds schematically to the water solvent relaxation in Fig. 1 in the excited state as equilibrium with the newly formed neutral solute is established; in contrast, the virtual work involved in the calculation of the corresponding frequency shift is that associated with the schematic charged solute, ground state “uphill” passage from A to B in Fig. 1. A general feature of the virtual work contributions in Fig. 2 is the dominant role of water librations/rotations over translations; this is remarkably similar to the situation found for the real work contributions for the neutral to charged solute transitions discussed at length in I. So far, no approximation is made (beyond that in the basic models); this is taken up next.

### C. Approximation of Virtual Coulomb Energy Fluxes by Real Fluxes

As extensively discussed in Sec. III A, and by design especially highlighted by our extreme illustration in Sec. III B, the nonequilibrium average work involved in the calculation of the frequency shift and the contributions to that work can be virtual rather than real and not be a rigorous representation of the true dynamics involved. In our  $q = 1 \rightarrow q = 0$  example of Sec. III B, the actual dynamics involve the water solvent relaxing in the presence of the neutral, excited state solute, having started (after excitation) from a nonequilibrium initial distribution dictated by the original, unexcited charged ground state solute (schematically the top portion of Fig. 1). But the average work whose calculation mathematically gives the shift according to Eq. 13 is a virtual work  $-W^{gs|es}(t)$  associated with different dynamics: the interaction of the ground state charged solute with the solvent evolving on the excited state, i.e. in the presence of a neutral solute (schematically the bottom portion of Fig. 1 from A to B). To be explicit, for the virtual work, the water solvent is evolving from equilibrium with the  $gs$  charge  $q = 1$ —which is a nonequilibrium state for the  $es$  charge  $q = 0$ —to a nonequilibrium state for this  $gs$  charge  $q = 1$ , which is the equilibrium state for the  $es$  charge  $q = 0$ ; this entire “uphill” evolution occurs in the presence of the  $es$  charge  $q = 0$ .

And—as we have discussed—it is of considerable interest to have a reasonable, nonequilibrium average real work, approximation for such a virtual work  $W^{gs|es}(t)$ , particularly in connection with the decomposition of the work in terms of contributions from the solvent molecular librations and translations. For the  $q = 1 \rightarrow q = 0$  example, this is the approximation  $W^{gs|es}(t) \sim -W_{inv}^{gs|gs}(t)$  in Eq. 13: in the approximated average work contribution the water solvent relaxes—from an initial condition equilibrated to the excited state neutral solute—but now in interaction with the ground state charged solute, i.e. with its dynamics determined by the interaction with the ground state charge. The relaxation completes with establishment of solvent equilibrium with the charged ground state solute. All this is schematically the bottom portion of Fig. 1 from B to A. In the language of the preceding paragraph,  $W_{inv}^{gs|gs}(t)$  is associated with the water solvent evolving from a nonequilibrium state for the  $gs$  charge  $q = 1$ —which is an equilibrium state for the  $es$  charge  $q = 0$ —to the equilibrium state for the  $gs$  charge  $q = 1$ —which is a nonequilibrium state for the  $es$  charge  $q = 0$ . This entire “downhill” evolution, or relaxation, occurs in the presence of the  $gs$  charged solute  $q = 1$  (indeed, the magnitude of this average work determines the frequency shift for the  $q = 0 \rightarrow q = 1$  excitation/relaxation process studied in I). A simple sign reversal in Eq. 13 between this real work and the virtual work above to compensate for the reversed direction does not establish equality between them: the dynamics are not the same since the charge actually present and

governing the dynamics is not the same.<sup>11,33</sup>

This real work  $W_{inv}^{gs|gs}(t)$  and its decomposition are in fact directly available from our results in I (see Figs. 3 and 5 in I), in particular, the simulation results for the  $q = 0 \rightarrow q = +1$  transition (the ground and excited state labels are reversed in I compared to the present case, but this affects neither the physics nor the numerical results); thus, the virtual work/real work comparison can be immediately accomplished.

Figure 3 displays this comparison. For convenience, we display both the virtual and its real work approximation in a relaxation perspective (i.e., B to A in Fig. 1): the real work contributions are the results for the  $q = 0 \rightarrow q = +1$  transition in Fig. 5a of I ( $W^{es|es}$ ) and the solid lines are the negative of the ground state virtual work contributions in Fig. 2 ( $-W^{gs|es}$ ). We first remark that at long times in Fig. 3, the Coulomb energy increments (red curves) tend to the same value, becoming indistinguishable at times larger than 1 ps (not shown). This occurrence is in good accord with the supporting argument given at the end of Sec. III A, according to which on average these energies should not depend significantly on the set of trajectories used.

But the most relevant aspect of Fig. 3 is that as expected, the nonequilibrium average time-dependent behavior of the work contributions and the Coulomb energy is not identical for the virtual and real cases. However, the quantities are similar enough that the real work  $W_{inv}^{gs|gs}(t)$  contributions involved in the relaxation after the neutral *es* solute has made a transition to its ground state (B to A in Fig. 1)—involving the charged *gs* solute and *gs* dynamics— provide a reasonable approximation for the “virtual” fluxes contributing to the virtual work  $W^{gs|es}$  computed for the *gs* charged solute interacting with the water solvent whose dynamics is determined by interaction with the neutral *es* solute. While there are clear accords in the dominance of water libration/rotation over translation for the energy flow and for the oscillation frequencies and phasing, there are noticeable relaxation time scale differences: e.g. in Fig. 3 the energy gap solvent relaxation (red curves) is faster in the virtual work case. (A related effect was observed by Maroncelli and Fleming,<sup>17</sup> a point we return to in Sec. IV B ).

#### IV. A COMPLEMENTARY APPROACH: TOTAL WORK

##### A. General features

The previous discussion has emphasized the insight provided by solute-solvent Coulomb energy fluxes, and how these naturally arise in the computation of the experimentally measurable time-dependent frequency shift. But we have seen in Sec. III that an important limiting aspect is that in some cases this sort of analysis fails to provide a complete account. This limitation was high-

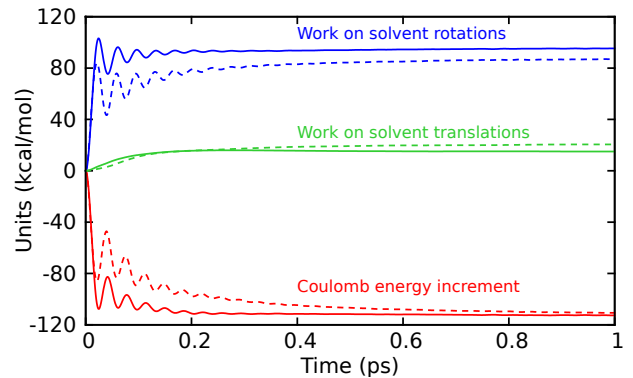


FIG. 3: Comparison of the nonequilibrium average Virtual work contributions and their Real work approximations; the perspective adopted is that of relaxation. We suppress the overbar notation for averages in this caption. The solid curves display the (negative of) the nonequilibrium average results in Fig. 2 for the virtual work case associated with the ground state, e.g. the  $+W^{gs|es}(t)$  contribution to the frequency shift for the  $q = +1 \rightarrow q = 0$  transition; the *gs* charge  $q = 1$  interacts with the water solvent which evolves from a nonequilibrium state for the *es* charge  $q = 0$  (equilibrium state for the *gs* charge  $q = 1$ ) to the equilibrium state for the *es* charge  $q = 0$  (nonequilibrium state for the *gs* charge  $q = 1$ ), with the dynamics being that of the *excited* state, with  $q = 0$ . The dashed curves display the corresponding contributions for its real work approximation  $W_{inv}^{gs|gs}(t)$ , the *gs* charge  $q = 1$  interacts with the water solvent which evolves from a nonequilibrium state for the *gs* charge  $q = 1$  (equilibrium state for the *es* charge  $q = 0$ ) to the equilibrium state for the *gs* charge  $q = 1$  (nonequilibrium state for the *es* charge  $q = 0$ ), with the dynamics being that of the *ground* state, with  $q = 1$ , see the text (the work on solute translation is excluded given its negligible role). As will be discussed in Section IV B, the two potential energy contributions correspond to the time dependence of the frequency spectral shift (see the second member of Eq.14), the solid line corresponding to  $1 \rightarrow 0$  and the dashed line to  $0 \rightarrow 1$ .

lighted in detail in Sec.III B for a charged solute that turns neutral when electronically excited. The natural expectation then is that the frequency shift function  $S(t)$ , Eq. 5, directly reflects the system’s dynamics on the excited electronic state where the solute has become suddenly neutral. Instead, this function contains information strictly limited to the virtual, rather than real, solute-solvent work associated with the ground electronic state charged solute in interaction with the solvent dynamics of the excited state. While we were able to show a ground state, real work approximation was useful in this case, there is an important point to be made here. Attention to the work directly involved in  $S(t)$  is of obvious importance since  $S(t)$  is experimentally observable; but constraining attention solely to that function clearly limits our understanding of the whole process.

Bypassing this difficulty is possible once the focus is shifted away from its exclusive focus on the frequency shift, and can in fact be accomplished during the compu-

tation of  $S(t)$  without any increase in complexity or computation time. One possibility is to track *total* Coulomb energy, but a choice which directly involves all the interactions is preferable, and is the one followed here. This more general choice is that of the total potential energy, i.e. to include Coulomb interactions and short range (e.g. Lennard-Jones) interactions; this has the critical advantage that variations in total potential energy will be directly translated into actual kinetic energy changes, which are often more easily interpretable. From a more practical standpoint, this choice comes with the additional bonus that the total force required can easily be obtained from the basic output of Molecular Dynamics simulation packages.

With our focus on the total potential energy, the power and work equations corresponding to those of Sec. III A are completely straightforward (and apply for individual trajectories and nonequilibrium averages). Now the Hamiltonian is simply

$$H = K + U, \quad (18)$$

where the potential energy function  $U$  will depend on whether we are studying dynamics on the excited or ground state relaxation, which should be analyzed separately. The time variation of  $U$  is simply the sum of the total powers on each site

$$\frac{dU}{dt} = - \sum_i \vec{F}_i \cdot \vec{v}_i, \quad (19)$$

so that its time increment equals (minus) the sum of the work contributions on each of the sites, which as in Sec. III A can be partitioned into work on rotations and translations (for rigid solvent). The total potential energy's variation will equal as well minus the total variation in kinetic energy.

### B. Rotational/Translational contributions

As with the previous computations in this paper, we start from a set of equilibrated configurations for a neutral or charged solute in water. At  $t = 0$  the solute charge is changed in the modeled electronic transition and a corresponding set of nonequilibrium trajectories is followed in time. The energy and work quantities just described are computed and averaged, with the results to be shown corresponding to sets of 1000 trajectories, each 2.5 ps long, with a 0.2 fs time step.

Two cases will be compared to highlight the basic issues involved: (a) the transition  $q = +1 \rightarrow q = 0$  (the extreme example choice of Sec. III B), for which the analysis of total energy is mandatory if we want to obtain information about the dynamics on the excited neutral solute state; (b) the transition  $q = 0 \rightarrow q = +1$ , where an analysis of the ion-solvent Coulomb energy fluxes has already provided a quite satisfactory picture (see I). In contrast to the situation for the solute-solvent potential

energy considerations of Sec. III, here the total potential energy increments  $\Delta U(\infty)$  will not be necessarily equal in these cases: in case (a) the water evolves to come to equilibrium with the newly created neutral solute, while in case (b) it must equilibrate to a newly created charged solute. The basic results are displayed in Fig. 4.

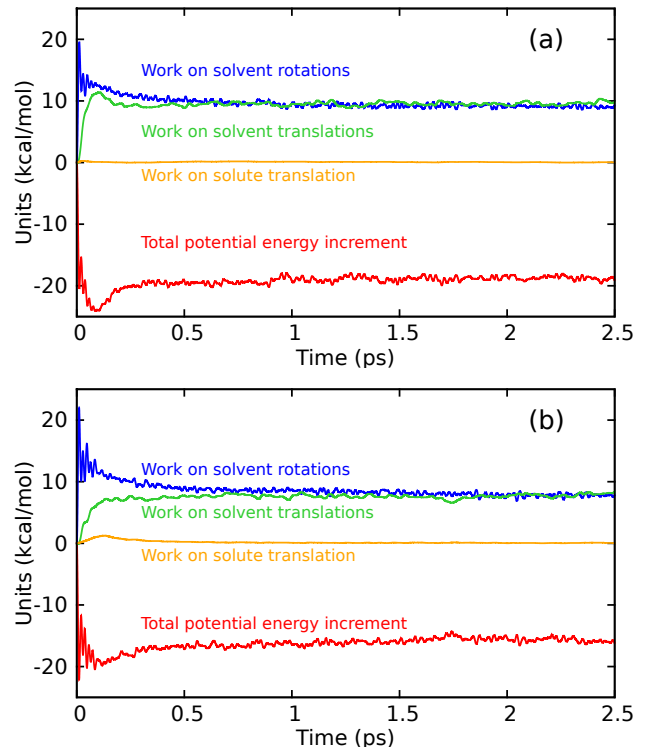


FIG. 4: Nonequilibrium relaxation functions for two solute excitation cases in water solvent, related to the monitoring of the average solute-solvent system's total potential energy, see Eq. 19. (a)  $q = +1 \rightarrow q = 0$ ; (b)  $q = 0 \rightarrow q = +1$ .

A noteworthy feature, that contrasts with corresponding results in Sec. III C, is that the work on water solvent translations and librations tends to the same value at long times in both cases. This naturally follows from the fact that here the work performed by the total force is equal to the total kinetic energy increment; since the rotational and translational kinetic energies—which have the same number of degrees of freedom—should be increased by the same amount from their initial equilibrium values, since equipartition will hold when equilibrium with the new solute charge is reached.

It must be recognized that, in the present, more coarse-grained point of view, some specific information is lost. In contrast with Sec. III, which focused on specific ion-water Coulomb forces, the emphasis is now on the accumulated work on each mode, which stems from the forces from all molecules in the sample. This specificity in Sec. III resulted in a plateau for the contributions of the work on each mode (see Fig. 3). These contributions accounted for the work exerted by a charged solute on translations/rotations of its neighbors, and this plateaus

in time since excess energy spreads into the whole sample instead of returning to first shell ion-water pairs. For the functions displayed in Fig. 4, the plateaus reached here reflect the attainment of equilibrium. They result from the ongoing exchange of energy between all molecules, in particular the excess energy initially deposited into water rotations is very rapidly transferred into neighboring molecule rotations and to a lesser degree into their translations, an issue discussed in detail in Ref. 16.

We pause to remark that we could have of course focused on the interaction energy between the water molecules of the first shell and the rest of the aqueous solvent. While this route could certainly be of interest in particular cases, we have not pursued this more complex approach since we believe that tracking the total energy is already quite informative, with the advantage that the equality of translational/rotational work discussed above provides an unambiguous signal of equilibration.

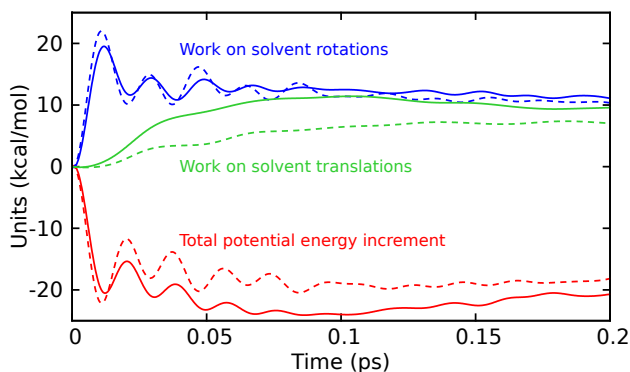


FIG. 5: Comparison of nonequilibrium average excitation/relaxation quantities for reverse solute excitation cases in water solvent. Solid lines:  $q = +1 \rightarrow q = 0$ ; dashed:  $q = 0 \rightarrow q = +1$ . (The negligible work on the solute translation is not displayed.)

The most important aspect of the comparisons in Fig. 4 are more clearly revealed in the shorter timescale version Fig. 5. Scrutiny of the real energy fluxes for the charge extinction and creation cases indicates that, at the very shortest times in Fig. 5, there is very little difference in the magnitudes and time scales of the dominant contribution, that of the work on water solvent librations.

The value of the total energy flux perspective can be examined in a more detailed context. To place this examination in proper perspective, we require a somewhat extended preamble, and to introduce that we need to first recall that, in our Section III C discussion of Fig. 3, we noted the noticeable differences in the relaxation time scales for the charge extinction and creation cases, and pointed out a related result in the pioneering Maroncelli and Fleming (MF)<sup>17</sup> aqueous solvation dynamics study, for the same solute-solvent systems used here. As Fig. 3's caption notes, the potential energy increment curves there exhibit the time dependence of the frequency shift function  $S(t)$  in Eq. 11. The numerical results in Fig. 3

and in MF<sup>17</sup> are qualitatively similar in reflecting more rapid dynamics for the charge extinction case; but they do differ quantitatively, since e.g. the water potentials used are different.

MF attributed<sup>17</sup> the more rapid dynamics to the special  $q = 1 \rightarrow 0$  case effect of the sudden repulsion—and consequent rapid water reorientation and spatial expansion—generated between closely separated water molecules, when the strong solute-water molecule attractive Coulomb forces disappear after excitation. This repulsion effect involves real forces and work, but as emphasized in Secs. III B and III C, the charge extinction case's frequency shift is governed by the virtual work  $W^{gs|es}(t)$ ; and this work involves the  $gs$  solute charge  $q = 1$  interacting with the water solvent, whose dynamics is governed by the  $es$  neutral solute  $q = 0$ , which is a situation not actually occurring in the charge extinction case. Yet this does not necessarily exclude the basic MF-invoked effect. After all,  $W^{gs|es}(t)$  involves the water solvent dynamics in the uncharged solute's presence, starting from the solvent's initial equilibrium with the  $gs$  charged solute; any repulsion-related effect in the water solvent would influence the monitored solvent—(not actually present)  $gs$  charged solute Coulomb interaction energy.

Nonetheless, we wish to consider real work and energy associated with the excitation/relaxation solvation dynamics as a probe of the dynamics. The approximation  $W_{inv}^{gs|gs}(t)$ , seen in Fig. 3 to do a reasonable job, does not help us here;  $W_{inv}^{gs|gs}(t)$  does not involve the  $es$  dynamics at all, thereby excluding any dynamic expansion, and so is silent on the effect's reality.<sup>33</sup> After all this provision of perspective, we can now finally consider what our alternate, total energy perspective says about this rapid solvent expansion/relaxation dynamics issue. The story can be relatively brief, since we have reviewed the basic librational and translational dynamics of Figs. 4 and 5 already above. We focus only on the shorter time Fig. 5, which is the most pertinent. This shows that the energy transfer involved is very nearly the same for the water librations and so that the difference is dominated by the transfer to the water translational motions. This lends some support to the MF repulsion hypothesis for the water translations but not for the water librations, although it must be emphasized again that the water models in the present and MF studies are different. Clearly a direct explicit examination of the motions involved would be of interest here, and will be pursued separately. But we can say here that, with the presently employed SPC/E water potential, the relative rapidity of the relaxation for the charge extinction case compared to the charge creation case is seen in Fig. 5 to arise from the larger amplitude, and faster, real work contribution of the energy flow into the water solvent translational degrees of freedom.<sup>34</sup> This completely real work analysis explicitly accounts—in a fashion not possible from Sec. III analysis—for real trajectory events responsible for the relaxation speed disparity between the charge extinction and creation cases.

We now turn in Fig. 6 to analogous charge extinc-

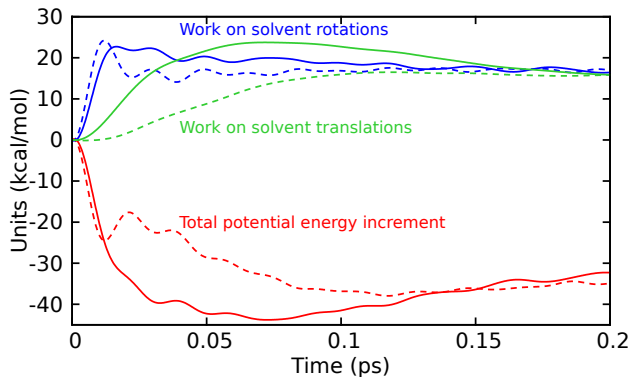


FIG. 6: Excitation/relaxation nonequilibrium average quantities involving a negatively charged solute in water, either for the ground electronic state or the excited electronic state. Solid lines:  $q = -1 \rightarrow q = 0$ ; dashed:  $q = 0 \rightarrow q = -1$ . (The work on the solute translation not included.)

tion/creation situations, except now with a negatively, rather than positively, charged solute. The motivation for this is the following. The common features for each excitation/relaxation in Figs. 2 and 5—an initial ultrafast work on rotations (blue curves), followed by a slower work on translations (green), with most of the excess energy redistribution achieved in  $\approx 200$  fs—indicate that in this new perspective the dominant role of work on rotations at short times found in Sec. III from the Coulomb interaction perspective is still visible (although at longer times both channels equilibrate, as previously discussed). The potentially general character of this mechanistic feature was already suggested in I from the solute-solvent Coulomb energy viewpoint.

We can pursue this generality issue by comparing in Fig. 6 excitation/relaxation cases involving a negatively charged solute:  $q = 0 \rightarrow q = -1$  and  $q = -1 \rightarrow 0$ . Again, a short time dominance of work on water librations is seen, with very little difference between the cases. The only significant difference is a faster appearance of the work on translations for the charge extinction case, a feature that also occurred with a positively charged solute. The analysis of structural changes accompanying these and other energy transfers in this paper will be reported elsewhere.

### C. Hydration Shell participation

The important issue of the extent to which the solvation relaxation has a collective nature—already examined in I in terms of solute-water solvent Coulomb energy—is now analyzed in terms of our new total energy perspective. Figure 7 displays the results for two neutral/positive ion cases, employing the hydration shell definitions detailed in Sec. II. We stress at the outset that the new total energy perspective allows these two cases to be compared on the same footing; recall

from Sec. III A that this was not possible from the solute-solvent Coulomb work perspective, since for the case  $q = 1 \rightarrow q = 0$  no solute-solvent interaction Coulomb energy exists on the excited state that could be monitored.

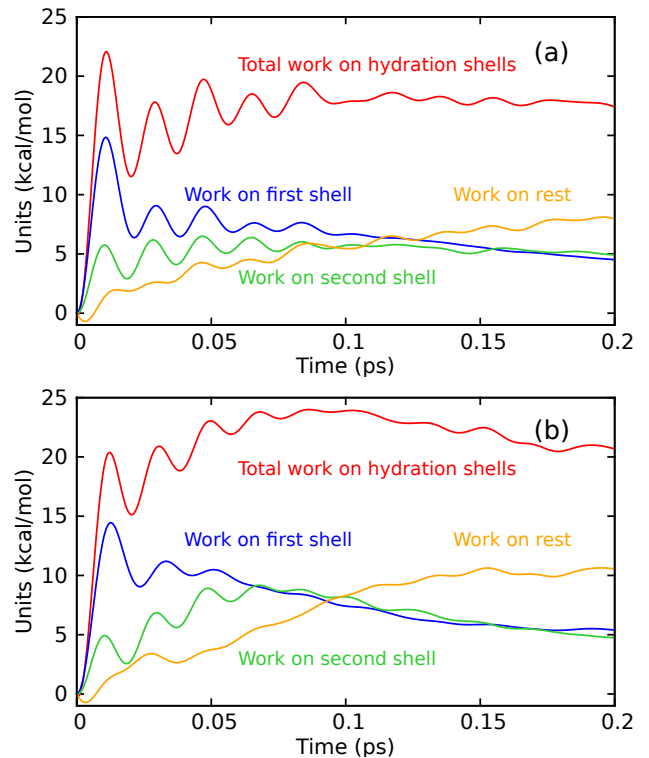


FIG. 7: Nonequilibrium average work on the different hydration shells for the neutral/positively charged solute cases: (a)  $q = 0 \rightarrow q = 1$ ; (b)  $q = 1 \rightarrow q = 0$ .

Figure 7 shows—not unexpectedly—a dominant role of the first shell, comprising 8 water molecules, at very short times, less than  $\sim 30$  fs. The work on the second hydration shell and on the rest of the water solvent is slower and less important, even though it comprises many more waters than the first shell. It is not until after approximately 100 fs that the work on the three defined zones is almost of the same magnitude; this is the point after which total work on molecules outside the first two hydration shells starts to dominate. Aside from somewhat more pronounced oscillations in the case of the neutral to charged solute excitation, no significant qualitative difference is observed between the two cases.

In the context of any “collective” behavior, we can say that the short time behavior indicates a dominant and strong participation of the first hydration shell waters, with the second shell waters evidently mainly responding to the perturbation of those water molecules, an effect that cascades into the third shell. This indicates that any collective effect that exists is fairly well localized to the first hydration shell.

#### D. Water rotational axes contribution

Finally, we turn to the participation of the water molecule rotational axes in the production of librational energy, now addressed via the present approach. The analysis in I for the cases  $q = 0 \rightarrow q = \pm 1$  clearly showed a dominance of work on rotations around the water molecule's lowest inertia moment axis. Figure 8 for the  $q = 0 \rightarrow q = 1$  case, and Figure 9 for  $q = 1 \rightarrow 0$ , display in the new total energy perspective the results for both the first and second hydration shells at short times. We see that the initial behavior up to 20 fs shows an ordering similar to that found in I, i.e. in the first hydration shell panel (a), most of the work is on the water's  $x$  axis followed by the  $z$  and  $y$  axes, a behavior also displayed in the second shell panel (b).

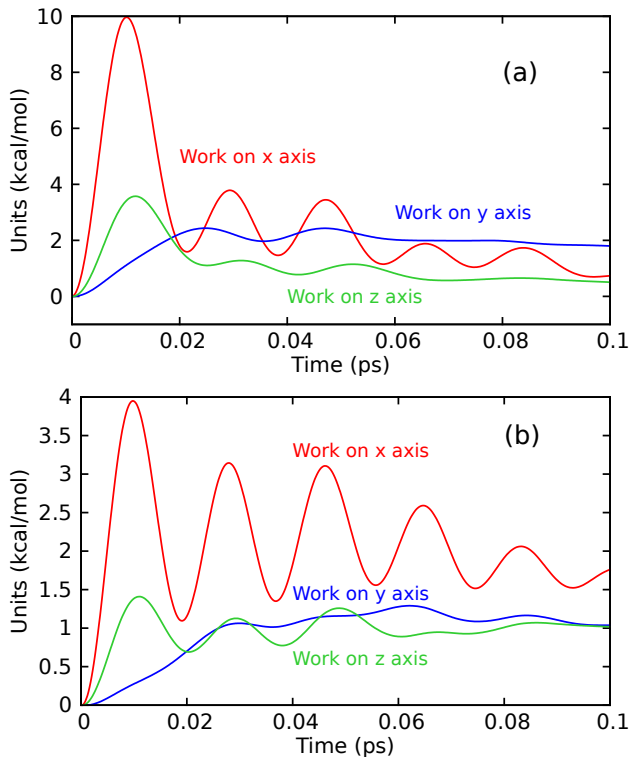


FIG. 8: Nonequilibrium average work on water molecule rotation for the case  $q = 0 \rightarrow q = 1$  and different body fixed rotational axes: (a) First shell ; (b) Second shell.

#### V. CONCLUDING REMARKS

A detailed analysis of energy fluxes turns out to be a powerful and flexible tool to understand the nonequilibrium relaxation pathways activated after solute electronic excitation in solution. When formulated in terms of the solute-solvent work, these contributions can be partitioned into energy fluxes into the different molecules/shells. It is shown however that this analy-

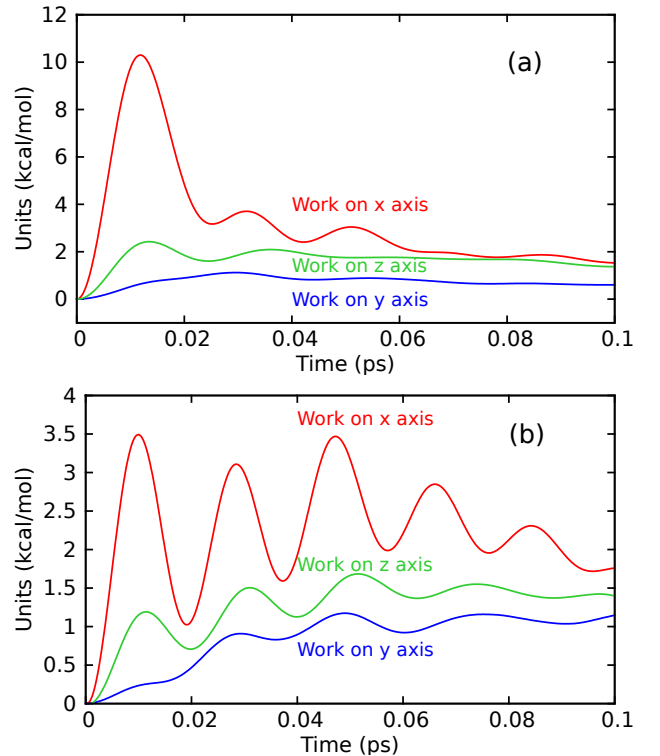


FIG. 9: Nonequilibrium average work on water molecule rotation for the case  $q = 1 \rightarrow q = 0$  and different body fixed rotational axes: (a) First shell ; (b) Second shell.

sis reveals that in some cases, the well-known frequency shift relaxation function  $S(t)$ , Eq. 6, is related not to a real work but rather to a virtual work, where the solute-solvent interaction is monitored for one electronic state while the dynamics per se are those involving a different electronic state. This situation is discussed via an extreme example of a solute's excitation in water, and it is indicated how an approximation can be usefully applied to connect the relaxation to real work terms.

In order to more directly deal with real work associated with actually occurring processes, a more general total energy perspective—which is not constrained to the frequency shift function  $S(t)$ —is developed and shown to provide an alternative viewpoint allowing detailed examination of the actual dynamics occurring during relaxation processes induced by solute electronic excitation.

In the present work and in I, since the aim has been basically exploratory, the solutes studied are extremely simple—neutral/charged monoatomic solute—(although the water solvent is not). But here and in I, a number of common trends exist, related e.g. to the initial dominance of energy transfer to water rotations, to the early dominance of first hydration shell energy reception, and to the dominance of energy transfer into the water molecule's rotational axis with the lowest moment of inertia. These common features' existence suggests their possible occurrence for the more realistic case of electronic excitations in polyatomic solutes with more gen-

eral charge distributions, an issue to be examined in future efforts.

CHE-1112564 (JTH).

### Acknowledgments

This work was supported by DGR (2009-SGR-1003) and MICINN (FIS2012-394-C02-01)(RR), and NSF grant

- 
- \* Electronic address: [rosendo.rey@upc.edu](mailto:rosendo.rey@upc.edu)  
 † Electronic address: [hynes@spot.colorado.edu](mailto:hynes@spot.colorado.edu)
- <sup>1</sup> Rey, R.; Hynes, J.T. Solvation dynamics in liquid water. I. Ultrafast energy fluxes. *J. Phys. Chem. B*, **2015**, DOI: 10.1021/jp5113922.
  - <sup>2</sup> Bagchi, B. Dynamics of Solvation and Charge-Transfer Dynamics in Liquids. *Ann. Rev. Phys. Chem.* **1989**, *40*, 115-141.
  - <sup>3</sup> Maroncelli, M.; Macinnis, J.; Fleming, G.R. Polar-Solvent Dynamics and Electron-Transfer Reactions. *Science* **1989**, *243*, 1674-1681.
  - <sup>4</sup> Fleming, G.R.; Wolynes, P.G. Chemical Dynamics in Solution. *Phys. Today* **1990**, *43*, 36-43.
  - <sup>5</sup> Fleming, G.R.; Cho, M.H. Chromophore-Solvent Dynamics. *Ann. Rev. Phys. Chem.* **47**, *47*, 109-134.
  - <sup>6</sup> Cho, M.; Fleming, G.R. Electron Transfer and Solvent Dynamics in Two- and Three-State Systems. *Adv. Chem. Phys.* **1999**, *107*, 311-370.
  - <sup>7</sup> Nandi, N.; Bhattacharyya, K.; Bagchi, B. Dielectric Relaxation and Solvation Dynamics of Water in Complex Chemical and Biological Systems. *Chem. Rev.* **2000**, *100*, 2013-2045.
  - <sup>8</sup> Maroncelli, M. The Dynamics of Solvation in Polar Liquids. *J. Mol. Liq.* **1993**, *57*, 1-37.
  - <sup>9</sup> Stratt, R.M.; Maroncelli, M. Nonreactive Dynamics in Solution: The Emerging View of Solvation Dynamics and Vibrational Relaxation. *J. Phys. Chem.* **1996**, *100*, 12981-12996.
  - <sup>10</sup> Bagchi, B.; Jana, B. Solvation Dynamics in Dipolar Liquids. *Chem. Soc. Rev.* **2010**, *39*, 1936-1954.
  - <sup>11</sup> Carter, E.; Hynes, J.T. Solvation Dynamics for an Ion Pair in a Polar Solvent: Time-Dependent Fluorescence and Photochemical Charge Transfer. *J. Chem. Phys.* **1991**, *94*, 5961-5979.
  - <sup>12</sup> Fonseca, T.; Ladanyi, B.M. Breakdown of Linear Response for Solvation Dynamics in Methanol. *J. Phys. Chem.* **1991**, *95*, 2116-2119.
  - <sup>13</sup> Leventhal, S.J.; Jimenez, R.; Fleming, G.R.; Kumar, P.V.; Maroncelli, M. Solvation Dynamics in Methanol: Experimental and Molecular Dynamics Simulation Studies. *J. Molec. Liquids*, **1994**, *60*, 25-56.
  - <sup>14</sup> Rey, R.; Ingrosso, F.; Elsaesser, T.; Hynes, J.T. Pathways for H<sub>2</sub>O Bend Vibrational Relaxation in Liquid Water. *J. Phys. Chem. A* **2009**, *113*, 8949-8962.
  - <sup>15</sup> Rey, R.; Hynes, J.T. Tracking Energy Transfer from Excited to Accepting Modes: Application to Water Bend Vibrational Relaxation. *Phys. Chem. Chem. Phys.* **2012**, *14*, 6332-6342.
  - <sup>16</sup> Petersen, J.; Møller, K.B.; Rey, R.; Hynes, J.T. Ultrafast Librational Relaxation of H<sub>2</sub>O in Liquid Water. *J. Phys. Chem. B* **2013**, *117*, 4541-4552.
  - <sup>17</sup> Maroncelli, M.; Fleming, G.R. Computer Simulation of the Dynamics of Aqueous Solvation. *J. Chem. Phys.* **1988**, *89*, 5044-5068.
  - <sup>18</sup> Perera, L.; Berkowitz, M.L. Dynamics of Ion Solvation in a Stockmayer Fluid. *J. Chem. Phys.* **1992**, *96*, 3092-3101.
  - <sup>19</sup> Roy, S.; Bagchi, B. Solvation Dynamics in Liquid Water. A Novel Interplay between Librational and Diffusive Modes. *J. Chem. Phys.* **1993**, *99*, 9938-9943.
  - <sup>20</sup> Nandi, N.; Roy, S.; Bagchi, B. Ionic and Dipolar Solvation Dynamics in Liquid Water. *Proc. Indian Acad. Sci. (Chem. Sci.)* **1994**, *106*, 1297-1306.
  - <sup>21</sup> Nandi, N.; Roy, S.; Bagchi, B. Ultrafast Solvation Dynamics in Water: Isotope Effects and Comparison with Experimental Results. *J. Chem. Phys.* **1995**, *102*, 1390-1397.
  - <sup>22</sup> Re, M.; Laria, D. Dynamics of Solvation in Supercritical Water. *J. Phys. Chem. B* **1997**, *101*, 10494-10505.
  - <sup>23</sup> Koneshan, S.; Rasaiah, J.C.; Lynden-Bell, R.M.; Lee, S.H. Solvent Structure, Dynamics, and Ion Mobility in Aqueous Solutions at 25 C. *J. Phys. Chem. B* **1998**, *102*, 4193-4204.
  - <sup>24</sup> Biswas, R.; Bagchi, B., Ion Solvation Dynamics in Supercritical Water. *Chem. Phys. Lett.* **1998**, *290*, 223-228.
  - <sup>25</sup> Tran, V.; Schwartz, B.J. Role of Nonpolar Forces in Aqueous Solvation: Computer Simulation Study of Solvation Dynamics in Water Following Changes in Solute Size, Shape and Charge. *J. Phys. Chem. B* **1999**, *103*, 5570-5580.
  - <sup>26</sup> Aherne, D.; Tran, V.; Schwartz, B.J. Nonlinear, Nonpolar Solvation Dynamics in Water: the Roles of Electrostriction and Solvent Translation in the Breakdown of Linear Response. *J. Phys. Chem. B* **2000**, *104*, 5382-5394.
  - <sup>27</sup> Rasaiah, J.C.; Lynden-Bell, R.M. Computer Simulation Studies of the Structure and Dynamics of Ions and Non-Polar Solutes in Water. *Phil. Trans. R. Soc. Lond. A* **2001**, *359*, 15451574.
  - <sup>28</sup> Duan, J.; Shim, Y.; Kim, H.J. Solvation in Supercritical Water. *J. Chem. Phys.* **2006**, *124*, 204504.
  - <sup>29</sup> Videla, P.E.; Rossky, P.J.; Laria, D. A Quantum Molecular Dynamics Study of Aqueous Solvation Dynamics. *J. Chem. Phys.* **2013**, *139*, 164506.
  - <sup>30</sup> Berendsen, H. J. C.; Grigera, J.R.; Straatsma, T.P. The Missing Term in Effective Pair Potentials. *J. Phys. Chem* **1987**, *91*, 6269-6271.
  - <sup>31</sup> Berendsen, H.J.C.; Postma, J.P.M.; van Gunsteren, W.F.; DiNola, A.; Haak, J.R. Molecular Dynamics with Coupling to an External Bath. *J. Chem. Phys.* **1984**, *81*, 3684-3690.
  - <sup>32</sup> The aspect of this approximation whereby the solute state and the associated solvent dynamics are made consistent bears a certain relationship to the two different forms of "linear response" approximations in an equilibrium time correlation function description of solvation dynamics<sup>11</sup>.
  - <sup>33</sup> In the context of our comments on approximations, we re-

mark that Maroncelli and Fleming<sup>17</sup> note that the sudden repulsion effect they invoke (discussed in the present MS's Section IV B) represents a departure, although not an extremely large one, from a linear response perspective.

<sup>34</sup> Unfortunately the net impact for the charge extinction case

of this faster translational contribution together with the comparable librational contribution is difficult to discern in the total potential energy increments in Figs. 5 and 6.